Original Article

Transformerless ANN-Controlled STATCOM-Based Power Quality Improvement for Three Phase DC-AC Boost Inverter in Grid-Connected Solar Photovoltaic Systems

J. Srinu Naick[1], G. Chandra Sekhar[2], K.V.R.B. Prasad[3], K. Hari Krishna[4]

[1,3]*Department of Electrical and Electronics Engineering, Chadalawada Ramanamma Engineering College, Andhra Pradesh, India.*
[2]*Department of Electrical and Electronics Engineering, GMR Institute of Technology, Andhra Pradesh, India.*
[4]*Department of Electrical and Electronics Engineering, Kallam Haranadhareddy Institute of Technology, Andhra Pradesh, India.*

[1]*Corresponding Author : speaksrinu@gmail.com*

Abstract - Power quality issues in grid-connected solar Photovoltaic (PV) systems are possible due to variations in sun irradiation and fluctuating loads. This study proposes a STATCOM-based power quality improvement system controlled by an Artificial Neural Network (ANN) for a three-phase DC-AC boost inverter to solve these issues. The proposed method comprises a solar PV array, a three-phase boost inverter, and the utility grid. Boost inverter voltage regulation and reactive power adjustment are supplied by the STATCOM. Unlike traditional STATCOMs, which rely on a transformer for isolation, the proposed system does not need one, reducing both the cost and complexity of the system. The control performance of the STATCOM is enhanced by using an ANN-based controller. STATCOM's control signals are trained using a backpropagation method to adapt to the current circumstances of the PV array and the grid. The ability to respond quickly and accurately to variations in solar irradiation and load fluctuations improves the power quality of the grid-connected PV system. Numerous studies have been devoted to the topic of power quality decrease using a variety of filters. Passive filters are one approach to improving power quality; however, they always cause some signal loss and have a constant amount of reactive power adjustment. Passive filters, which are often designed for specific frequencies, may not be able to sufficiently offset the power quality issues brought on by unexpected changes in load or harmonic distortions. Even passive filters have losses and require periodic maintenance. Simulations performed in the MATLAB/Simulink environment demonstrate the effectiveness of the proposed system in mitigating power quality issues such as voltage sags, swells, and harmonics. A stable and high-quality power supply is provided to the grid by the ANN-driven STATCOM, which successfully regulates voltage and compensates for reactive power.

Keywords - Power quality improvement, Grid-connected solar PV systems, STATCOM, Artificial Neural Network, Boost inverter, Reactive power compensation, Voltage regulation.

1. Introduction

Due to its benefits of being ecologically clean, pollution-free, and easy to install, renewable energy, led by solar power production, has gained attention on a global scale as the state of the environment worsens [1]. Large-scale grid-connected PV will be the primary form of photovoltaic power production, according to recent developments in the distributed solar energy generation system from the island to the integrated grid [2]. A converter connects the photovoltaic power-generating equipment to the low-voltage distribution network, enabling load power delivery. It can power neighbouring local loads when the light intensity is higher. The electricity grid supplies local loads when there is little light.

Typically, two-step converters are used in PV systems. While the low-voltage PV output is tuned and bucked or boosted appropriately at the first stage's DC-DC converter, the second stage's inverter converts the DC to a high-quality AC. These two-stage converters have numerous disadvantages despite their effective operation and direct manner, including their size, cost, level of dependability, and

weight. Several converters have been suggested in addition to this form of two-stage converter. [3] Due to source fluctuations, the two separate buck-boost converters for the two half cycles produce asymmetrical operation. Wang [4] offered another converter that utilises the buck-boost principle. However, there are several components used in the circuit configuration. In this study, the Voltage Source Inverter (VSI) shown in Figure 1, presented arrangement, known as a buck inverter, is most likely the most significant power converter scheme. It has several unique industrial and commercial uses. Among the most significant applications are AC motor drives and Uninterruptible Power Supplies (UPS).

One of the buck inverter's properties is that the instantaneous average output voltage always falls below the DC input value. Therefore, a boost DC-DC converter must be utilised between the DC source and inverter when an output voltage greater than the input voltage is required, as illustrated in Figure 2. The volume, weight, cost, and efficiency of this system might be considerable depending on the power and voltage levels involved. In this study, a brand-new VSI called a boost inverter is presented. Depending on the duty cycle, the boost inverter will naturally provide an output AC voltage that is either less than or greater than the input DC voltage [5-9]. The parts that follow include details on analysis, control, and experimentation. As shown in Figure 3, the proposed boost inverter converts DC to AC by differentially connecting the load across three DC-DC converters and modulating the output voltages of the converters sinusoidally. The Cuk converter has been used to explore this idea in [5, 6].

However, when integrating these devices with the utility grid, there are issues with power quality, efficiency, and cost-effectiveness. The conversion of DC electricity produced by solar PV panels into AC power that may be connected to the grid is made possible by inverter technology. Traditional inverters often use transformers for voltage transformation and isolation, which may complicate the system, increase costs, and result in efficiency losses. This research suggests a novel transformerless three-phase DC-AC boost inverter for grid-connected solar PV systems as a solution to these problems, as seen in Figure 3. A more compact, effective, and economical solution is produced by the transformerless design, which does away with the necessity for large, costly transformers.

The suggested inverter effectively transforms the DC power produced by the solar PV panels into grid-compatible AC power using cutting-edge power electronic methods. The inverter assures voltage boosting to meet the grid voltage needs by using a boost function, allowing easy interaction with the utility grid. Grid-connected solar Photovoltaic (PV) systems are gaining popularity as a renewable energy source that may help create a more sustainable and clean future.

However, there are issues with power quality, voltage control, and system stability when integrating these devices with the utility grid. The ability to convert solar panel-generated DC electricity into grid-compatible AC power is made possible by inverter technology. Traditional inverters often use transformers for voltage transformation and isolation; however, they may cause inefficiencies, space restrictions, and cost issues. This article suggests a novel strategy to overcome these problems by employing transformerless Artificial Neural Network (ANN) control for a DC-AC boost inverter in grid-connected solar PV systems [10, 11].

The transformerless design offers benefits in size, efficiency, and total system cost by doing away with the requirement for large, expensive transformers. The suggested transformerless DC-AC boost inverter uses cutting-edge electronic methods to turn DC power from solar panels into AC power coordinated with the grid. The inverter operation may be precisely and adaptively controlled by the system's ANN-based controller, improving power quality, voltage regulation, and system performance.

Many non-resistive loads connected to a large power grid may cause voltage distortion in the power grid at its end, three-phase imbalance, impact reactive power, and other unfavourable conditions that will negatively affect the distribution network [12-14]. These changes to the power grid and load, high-tech electronic products, and new challenges associated with the penetration of power electronics technology are all contributing factors. The conventional technique of compensating for reactive power involves employing devices like SVC, SVG, and STATCOM, which need extra investment in power equipment to correct for reactive power to enhance the voltage stability of the grid's terminals. Since the main components of the photovoltaic inverter and d-STATCOM are fully consistent according to research findings, photovoltaic power generation systems can be installed in distribution networks of terminals to supply reactive power; as a result, the study of the Voltage Source Converter (VSC) of grid-connected PV is crucial.

However, the voltage may be adjusted by dynamically switching reactive power at the feeder where solar farms are incorporated using flexible AC transmission system components such as the static voltage compensator. By reducing voltage flicker, providing power factor adjustment, and reducing steady-state overvoltage, the STATCOM may enhance the distribution system's performance [17, 18]. In contrast to STATCOM, which uses a VSC to exchange reactive power, PV systems employ voltage source converters to convert DC electricity to AC power. This shared characteristic of PV systems and STATCOM led to the creation of patent-pending technology that uses the PV inverter as STATCOM to regulate reactive power both

during the day and at night while producing actual electricity [15, 16]. This method may transport reactive electricity via existing PV systems without considering cost variations. The power transmission capacity was recommended to be increased using a special control of PV inverter, such as STATCOM. The idea of PV inverter control as STATCOM and investigations of the PVSTATCOM in MATLAB/Simulink are presented in this work.

2. System Layout

The utility grid provides the primary power source for a solar PV system that is linked to the grid. The PV array's AC electricity is sent into the utility grid, which helps power homes and businesses. To feed the PV array's DC electricity into the utility grid, a boost inverter must transform it into

AC power. It performs the required DC-AC conversion and amplifies the DC voltage to the required level. The STATCOM has various purposes and is included within the boost inverter, as shown in Figure 1.

To keep the grid voltage within safe parameters; it compensates for reactive power. It stabilises the voltage and prevents power quality problems, including dips, spikes, and harmonic distortion. The ANN controller's job is fine-tuning the DC-AC boost inverter's control signals. After being taught using a backpropagation method, it can make real-time adjustments to the control settings in response to changes in the PV array and grid state. The ANN controller's quick and precise answers to changes in solar irradiation and load improve the total control performance.
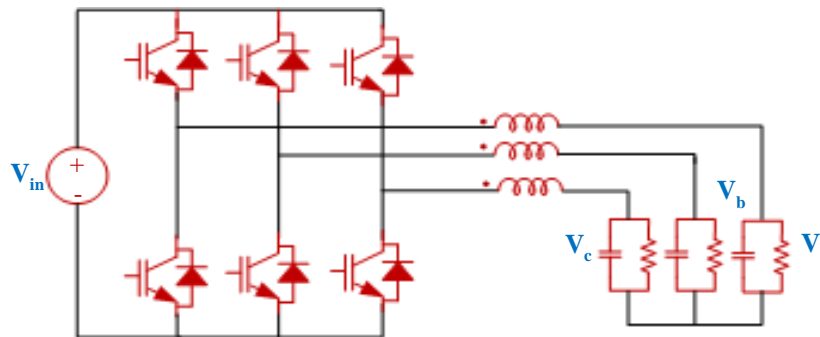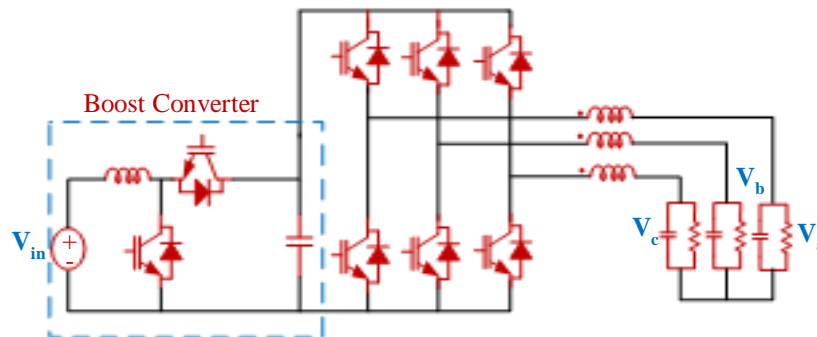

Fig. 1 Conventional buck-type inverter

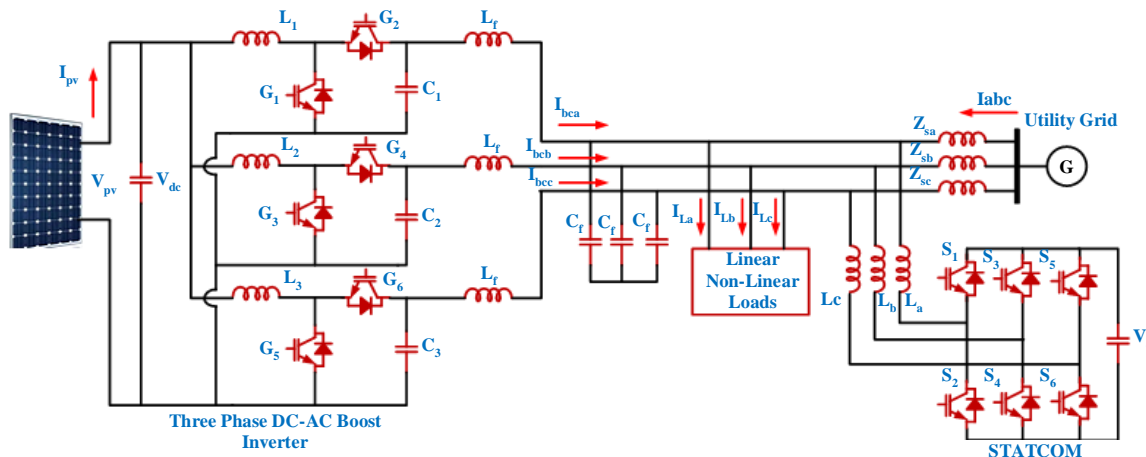**Fig. 2 Circuit used to generate an AC voltage larger than the DC input voltage**

Fig. 3 proposes a transformerless DC-AC boost inverter system setup

3. Design of Solar PV Array System

Solar PV panels may be integrated in parallel or series to construct the system. When solar PV panels are connected in series, the terminal voltage of the array rises, whereas when solar PV panels are connected in parallel, the current rating increases. Each panel is rated at 213.15 watts, with a maximum power point voltage of 29 volts, an open circuit voltage of 36.3 volts, a short circuit current of 7.84 amperes, and a maximum power point current of 7.35 amperes. There are ten PV panels in a series configuration and forty-seven in a parallel configuration. The full power point current is 345.45 A, and the maximum power point voltage is 350 V; the overall rating of the solar PV array is 30.837 kW; the PV panel voltage at the open circuit is 363 V; the PV current at the short circuit is 132.3 A; and so on. The solar PV array's power-voltage and current-voltage characteristics under varying irradiation circumstances are shown in Figures 4 and 5.
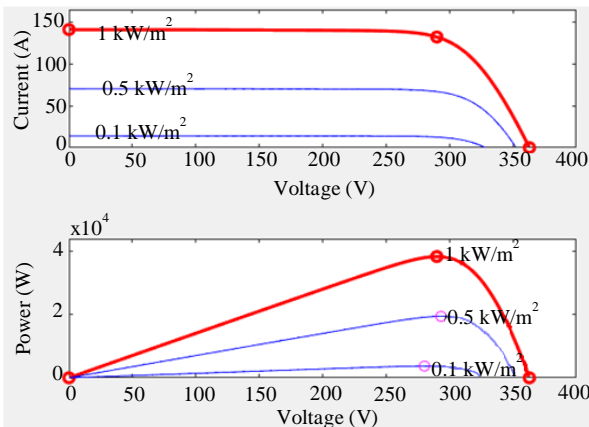

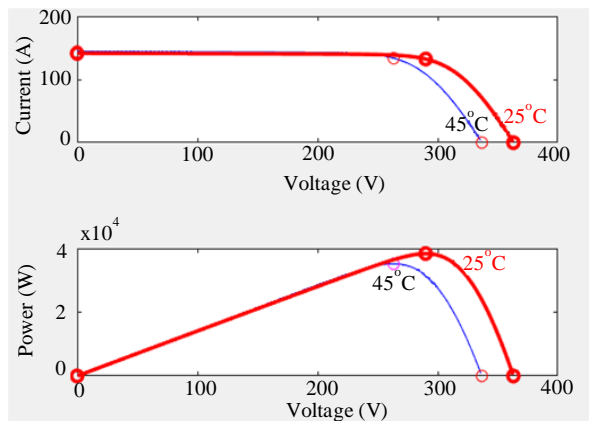**Fig. 4 Considered solar PV array's P-V and I-V properties for various irradiances**

Fig. 5 The P-V and I-V properties of the hypothetical solar PV array at different temperatures

4. Control Approach

4.1. Operation of Bidirectional DC-DC Buck Boost Converter

Switches S1 and S2 in a bidirectional DC-DC converter (shown in Figure 6) to choose between buck (step-down) and boost (step-up) operation. In both circumstances, let's examine how S1 and S2 swap modes:

4.1.1. Buck Mode Operation
- When S1 is activated, the higher voltage input source is connected to the lower voltage load. Through S1 and the inductor, current travels from the input source to the load.
- In this position, S2 is open, allowing current to flow in just one direction and blocking any attempts at reversal. It prevents the input source from receiving any energy from the output.
- The inductor behaves as follows: during the on period of S1, the inductor's magnetic field accumulates energy. During S1's off period, this power is transmitted to the load.
- The output voltage of a voltage converter operating in buck mode is less than the input voltage.

4.1.2. Boost Mode Operation
- When S2 is activated, the output load is connected to the input source (which has a lower voltage). The capacitor at the output is charged as current passes from the input source via the inductor.
- In this position, S1 is open, allowing current to flow in just one direction and blocking any attempts at reversal. This prevents any drain on the input power supply.
- The inductor behaves as follows: during the on period of S2, the inductor's magnetic field accumulates energy. During S2's off state, this power is transmitted to the output capacitor and load.
- When operating in boost mode, the output voltage is greater than the input voltage, representing a voltage conversion.

S1 and S2's duty cycles are modified in buck and boost modes to set the output voltage and manage the energy flow from the input to the load. The duty cycle is the fraction of a switching cycle that S1 is active compared to S2. Depending on the input and output voltage levels, bidirectional DC-DC converters may function in additional modes, such as buck-boost, where both step-down and step-up capabilities are used. A unique switching operation and control technique may be implemented depending on the converter architecture and the desired functionality.
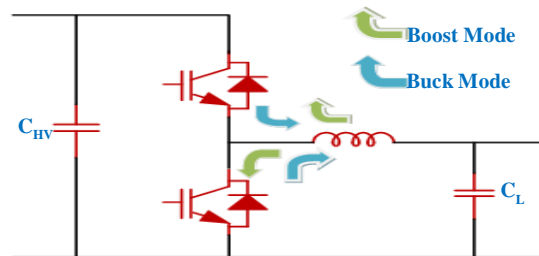

Fig. 6 Topology of a hard-switching bidirectional DC/DC converter, showing the direction of current flow during buck and boost operations

A bidirectional DC-DC buck-boost converter's inductor and capacitor values must be chosen per the converter's intended operating parameters and specifications. In a bidirectional buck-boost converter, these equations are often used to select the inductor and capacitor:

4.1.3. Inductor Selection

The converter's switching frequency, maximum current rating, and intended ripple current all play a role in determining the inductor value. Inductor values may be determined using the following formula:

$$L = \frac{(V_{out-max}*(1-D))}{\Delta I_L * f_s} \qquad (1)$$

Where, L = Inductor value, $V_{out-max}$ = Maximum output voltage, D = Duty cycle (ratio of on-time to the switching period), ΔI_L = Desired ripple current, f_s = Switching frequency.

4.1.4. Input Capacitor Selection

Input voltage ripple requirements and input voltage tolerances inform the input capacitor value. To get the value of the input capacitor, use the following formula:

$$C_{in} = \frac{(I_{in-max}*D)}{\Delta V_{in} * f_s} \qquad (2)$$

Where, C_{in} = Input capacitor value, I_{in-max} = Maximum input current, D = Duty cycle (ratio of on-time to the switching period), ΔV_{in} = Desired input voltage ripple, f_s = Switching frequency.

4.1.5. Output Capacitor Selection

The permissible output voltage variation and voltage ripple requirement establish the output capacitor value. The following formula determines the output capacitor value:

$$C_{Out} = \frac{(I_{out-max}*(1-D))}{\Delta V_{out} * f_s} \qquad (3)$$

Where, C_{Out} = Output capacitor value, $I_{out-max}$ = Maximum output current, D = Duty cycle (ratio of on-time to the switching period), ΔV_{out} = Desired output voltage ripple, f_s = Switching frequency.

4.1.6. Duty Ratio Calculation

Operating mode (step-up or step-down) and target output voltage determine the bidirectional buck-boost converter's duty ratio (D). The formulae for the duty ratios are as follows:

For step-up mode (D > 0): $D = 1 - \left(\frac{V_{in-min}}{V_{out-max}}\right)$

For step-down mode (D < 1): $D = \left(\frac{V_{out-min}}{V_{in-max}}\right)$

Where, D = Duty cycle (ratio of on-time to the switching period), V_{in-min} = Minimum input voltage, V_{in-max} = Maximum input voltage, $V_{out-min}$ = Minimum output voltage, V_{in-max} = Maximum output voltage.

4.2. Operation of Bidirectional Three DC-AC Boost Inverter

In [19, 20], a three-phase boost inverter is proposed. The figure shows that its primary parts are three series-coupled bidirectional boost converters. Each boost converter employs a DC-biased sinusoidal waveform with an adjustable duty cycle to generate a unipolar voltage greater than the input DC voltage.

The main advantage is that a three-phase AC output voltage is created with just six switches and a few small passive elements more significant than the input DC voltage. Figure 7 shows the results after the dc offset (Vdc) has been subtracted from the outputs of the two boost converters. Now we're down to simply the AC parts.

The following criteria characterise both individual converter outputs and their sum:

$$V_{aO} = V_{dc} + V_m \sin(\omega t) \qquad (4)$$

$$V_{bO} = V_{dc} + V_m \sin\left(wt - \frac{2\pi}{3}\right) \qquad (5)$$

$$V_{cO} = V_{dc} + V_m \sin\left(wt + \frac{2\pi}{3}\right) \qquad (6)$$

$$V_{dc} > V_m + V_{in} \qquad (7)$$

Where, V_{aO}, V_{bO}, and V_{cO} represent the boost converters' respective reference voltages. Following is how the line voltages at the output are calculated:

$$V_{ab} = V_{aO} - V_{bO} = \sqrt{3}V_m \sin\left(\omega t + \frac{\pi}{6}\right) \qquad (8)$$

$$V_{bc} = V_{bO} - V_{cO} = \sqrt{3}V_m \sin\left(\omega t - \frac{\pi}{2}\right) \qquad (9)$$

$$V_{ca} = V_{cO} - V_{aO} = \sqrt{3}V_m \sin\left(\omega t + \frac{5\pi}{6}\right) \qquad (10)$$
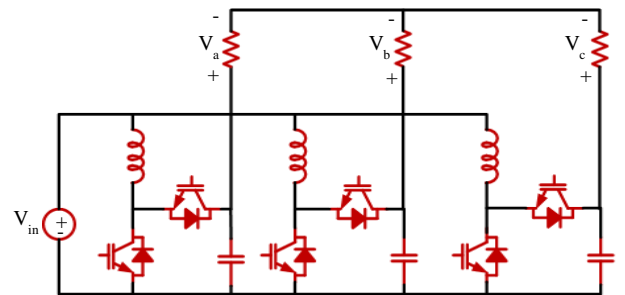

Fig. 7 A DC-AC boost converter is suggested. Therefore, the proposed three-phase boost inverter has balanced three-phase voltages at its load terminals

4.3. ANN Control Designing of DC-AC Boost Inverter

The DC-AC boost inverter is controlled by an ANN, which is trained using the procedures described in Section VI to give a reference signal and keep the voltage balanced across the DC link capacitor. The network is fed the difference between the reference voltage (350V) and the actual voltage (Vdc), together with the associated error, and the predicted output (i.e., the loss component of current) is provided as the target data. The 100-layer deep network is trained using Levenberg-Marquardt backpropagation. MATLAB/Simulink version of ANN model for capacitor voltage regulation (shown in Figure 8). The network, trained using Levenberg-Marquardt backpropagation, consists of 100 hidden layers. The Artificial Neural Network (ANN) model built in MATLAB/Simulink that generated the reference DC voltage is shown in Figure 8. Reference voltage and capacitor voltage balancing using an ANN control method: a MATLAB/Simulink model. Figure 9 compares the reference voltage generated by the ANN control system with the actual source voltage, which results in the shunt converter receiving the appropriate switching pulses. Voltage source converter switching PWM waveform.

4.4. D-STATCOM's Topology is Based on a Method for Carrier-Based PWM Control

The DC-link voltage to the network is provided by the inverter, transformer, and capacitor C that make up D-STATCOM. Power electronic IGBT converters are fully shown in D-STATCOM, a tool used for voltage management on the distribution network. The D-STATCOM regulates the voltage of the neighbouring bus by consuming or creating reactive power. Through the leaky reactance of the coupling transformer, reactive power may be transferred to the main feeder using a voltage-sourced PWM inverter [21]. Switching between inductance and capacitance operation is possible with D-STATCOM's DC link capacitor. When the bus voltage is lower than the reference voltage, D-STATCOM acts as a capacitor, releasing reactive power into the grid. Instead, when the bus voltage is higher than the D-STATCOM reference voltage [21, 22] and acts as an inductor, injecting positive reactive power into the grid. Figure 9 shows the D-STATCOM's many essential components. A capacitor provides DC power to the inverter and is connected to the LC-damped filters at the inverter's output. First, the current from the supply side is calculated, and then, using the measured voltage and current from the load side, the D-STATCOM compensatory current is calculated [21]. PWM pulses, used by the inverter bridge to track the reference voltage and monitor the input voltage, are created when the load current is subtracted from the compensating current. These voltage-sourced PWM inverters provide better control than single-bridge designs since they use two IGBT bridges. A twin inverter design generates fewer harmonics than a single bridge, which results in smaller filters and a quicker response time [23]. Two separate ANN regulators manage the voltage and current components supplied by the PLL's synchronous reference, which are calculated using sint and cost.

Figure 9 shows that four ANN controllers are in charge of the two current regulation loops (inner and outer). Two Artificial Neural Network (ANN) controllers handle the inner current regulation loop, one for the d-axis and one for the q-axis. The controller outputs the Vd and Vq voltages determined by the PWM inverter's pulse generator. Integrated outputs (Vd and Vq) from modern ANN controllers are converted to phase voltages (Vabc). The DC-link voltage regulation loop [23] provides reference Iq, whereas the external voltage regulation loop provides reference Id. The outer current regulation loop's other two ANN controllers, Iq reference and Id reference, are determined by calculating the delta between the value reference voltage and the measured voltage. As shown in Figure 9, the ANN controller's output sets the Id reference when the DC link voltage error is input and the Iq reference when the network side AC voltage error is input. It keeps the primary side's voltage stable at the selected level. A Pulse Width Modulation (PWM) generator may interact with and manage VSC Pulse IGBTs after determining Vq and Vd [24].
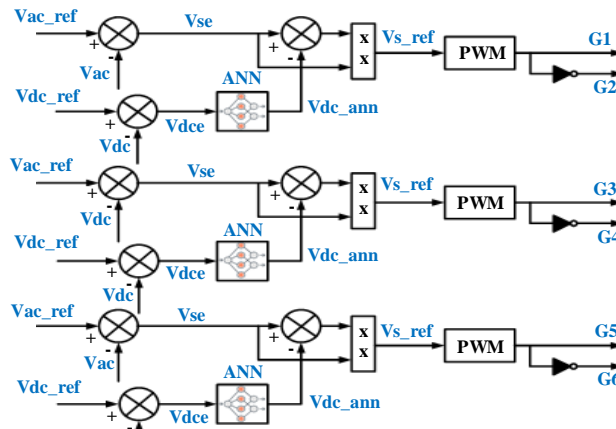

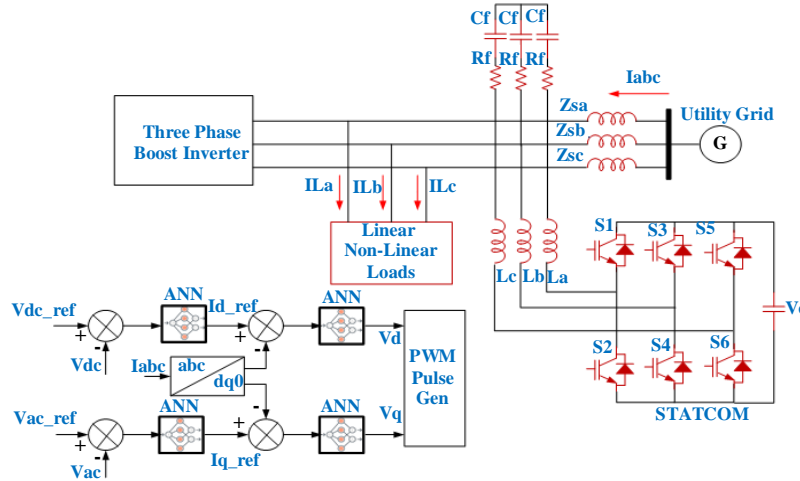
Fig. 8 DC-AC boost inverter system control design

Fig. 9 D-STATCOM topology for carrier-based control

5. Artificial Neural Network Scheme

AI development aimed to create software that could learn new abilities and reason like a human being. Artificial Neural Networks (ANN) are computer systems that use the same control strategy as biological neural networks. Input, hidden, and output layers make up the architecture of an ANN, as shown in Figure 10.

The ANN draws all of its operational data from the input layer. The input layer stores these inputs before sending them to the hidden layer for processing. The inputs are multiplied by the weights of the links between the input and hidden layers. The calculated outcomes are stored in the output layer depending on the bias applied to the hidden layers. Since ANN computes data in parallel instead of sequentially, it is much faster than conventional systems. There might be a wide variety of ANN architectures and learning rules. This research uses one of these approaches to generate voltage and current standards.

The most effective layout for electronics is a feed-forward error backpropagation network. The weights of the links are flipped if the ANN's outputs are incorrect; this is done so that, for a given input to that layer, the new weights process the data in a way that yields the anticipated outputs. Levenberg-Marquardt Backpropagation (LMBP) delivers faster convergence [25, 26] when the mean square error performance function is used during training. In contrast to the conventional error backpropagation method, this is a whole new approach. LMBP revises the weights based on the derivatives.
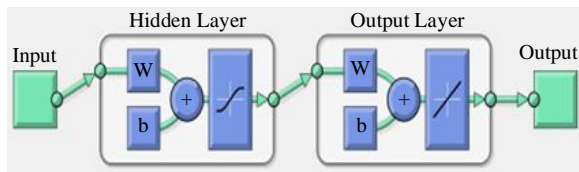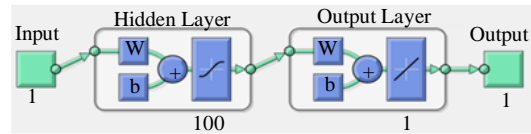

Fig. 10 Basic ANN structure

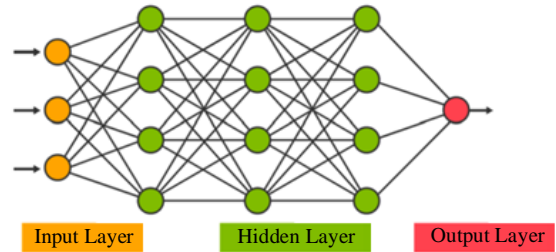**Fig. 11 Both the DC-AC boost inverter, and the shunt converter include an ANN framework**

Fig. 12 Design of a backpropagation network to provide a standard reference signal

5.1. The Design of the ANN Controller Using MATLAB/Simulink

Here, we describe the steps used in the MATLAB/Simulink environment to create an ANN controller:

- The nftool command is used to design and train a network, and then the mean square error and regression analysis are used to determine how well the network performed.
- The problem-defining input and output data are required to build the network.
- Neural network fitting tool allocates 70% of data to training by default. Here, 15% of the samples are utilised to verify the network's accuracy, 15% to assess the accuracy of the network, and 15% to stop training when generalisation no longer improves.
- The network's size varies depending on the number of hidden layers. The number of neurons may be adjusted if the trained network is underperforming.

- Levenberg-Marquardt Backpropagation (trainlm) will be used for the training process. Training is immediately terminated when the mean square error of the validation samples begins to rise, indicating that generalisation has stalled.
- A Simulink file may be made when training is finished.

6. Results and Discussion

The proposed grid-connected PV system shown in Figure 1 is modelled in this section using a transformerless VSC topology. A simulation has been developed to evaluate the effectiveness of the proposed control strategy in injecting the energy generated by the PV array and correcting for reactive power in local loads. The simulation takes 0.8s to complete. The sun irradiance reduces from 1000W/m^2 to 500W/m^2 in 0.5s in the no-STATCOM and STATCOM situations, with the temperature remaining at 25 degrees Celsius throughout.

The control system uses a sample time of 100 μs throughout the board, including in the PLL synchronisation unit, voltage controllers, and current controllers. The boost and VSC converter pulse generators, employ a 1μs sample period, guaranteeing clean PWM waveforms. The switching frequency of the IGBT has been set at 10 kilohertz. As previously stated, a PV array's maximum power output is 10,137 kW at 1000Wm^2.

When the amount of solar irradiation drops by half in a second, the amount of active power from PV output drops to 8.32 kW. (Figures 13, and 14) show that after stabilising the system, the PV modules' active power production follows a smooth curve. This demonstrates the correct operation of the PV ar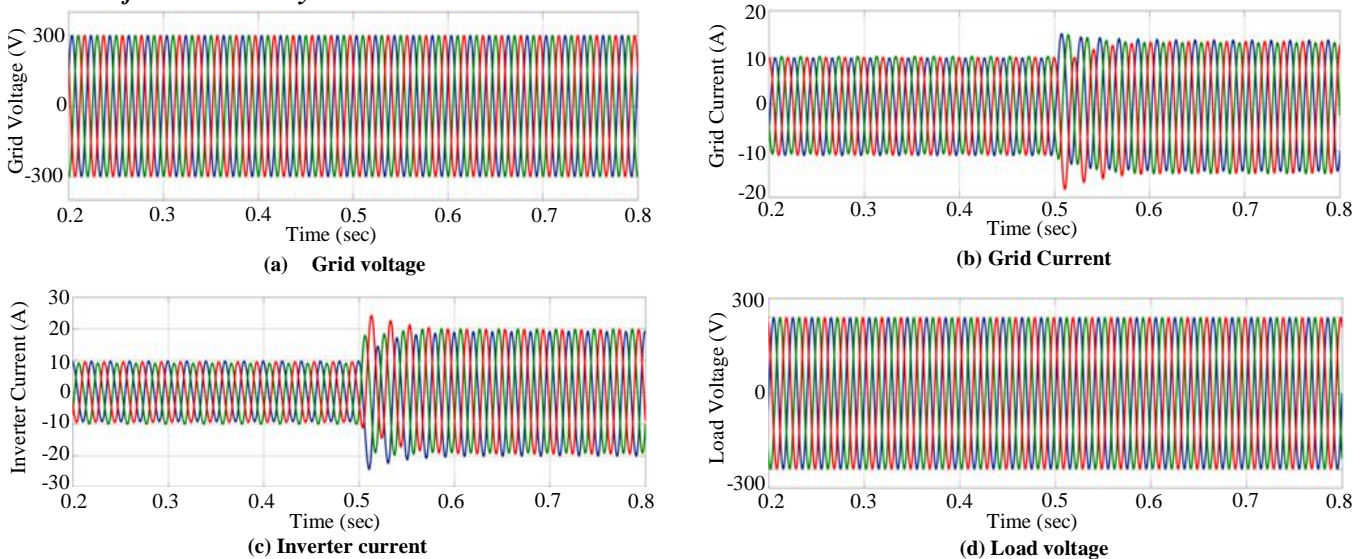ray model, and DC-AC boost inverter. (Figures 13, and 14) show active power as a continuous line and reactive power as a dashed line. Between 0.2s and 0.5s, when sun irradiation is at its strongest, VSC produces its maximum active power. It can handle the required dynamic electricity in the local area (8.74 kW).

The active power excess is nonetheless returned to the grid. This time period also demonstrates the efficiency of the control approach for adjusting local load reactive power by showing that VSC produces almost enough reactive power to fulfil the local load (2.167kvar). Due to a drop in solar irradiance, VSC's output drops to 50% of its maximum active and reactive power between 0.5s and 0.8s, far below local load needs.

However, the production of reactive power has undergone a little shift. It is also evident that the time it takes for the system to achieve a steady state is more than 0.2s. Between 0.2s and 0.5s, the DC link voltage stays constant. The DC connection voltage will fluctuate significantly as the sun's irradiance decreases at 0.5 seconds.

The Artificial Neural Network (ANN) control mechanism stabilises this deviation in about 0.2 seconds. It does the job, albeit more performance in terms of control is desirable. When solar irradiance is high, the PCC keeps the voltage where it should be. As solar irradiance drops, the voltage at PCC hardly climbs. A short process occurs with the change from one stable state to another. Curves of voltage in a three-phase system are smoother than those of current. When solar irradiance is high, keeping the current constant may also be possible. When solar radiation is low, there is less available power. The control algorithm can and should be improved since sunlight is the only variable to adjust.

6.1. Results for Grid Stability and Solar Power Generation under Variable Solar Irradiance without STATCOM Condition
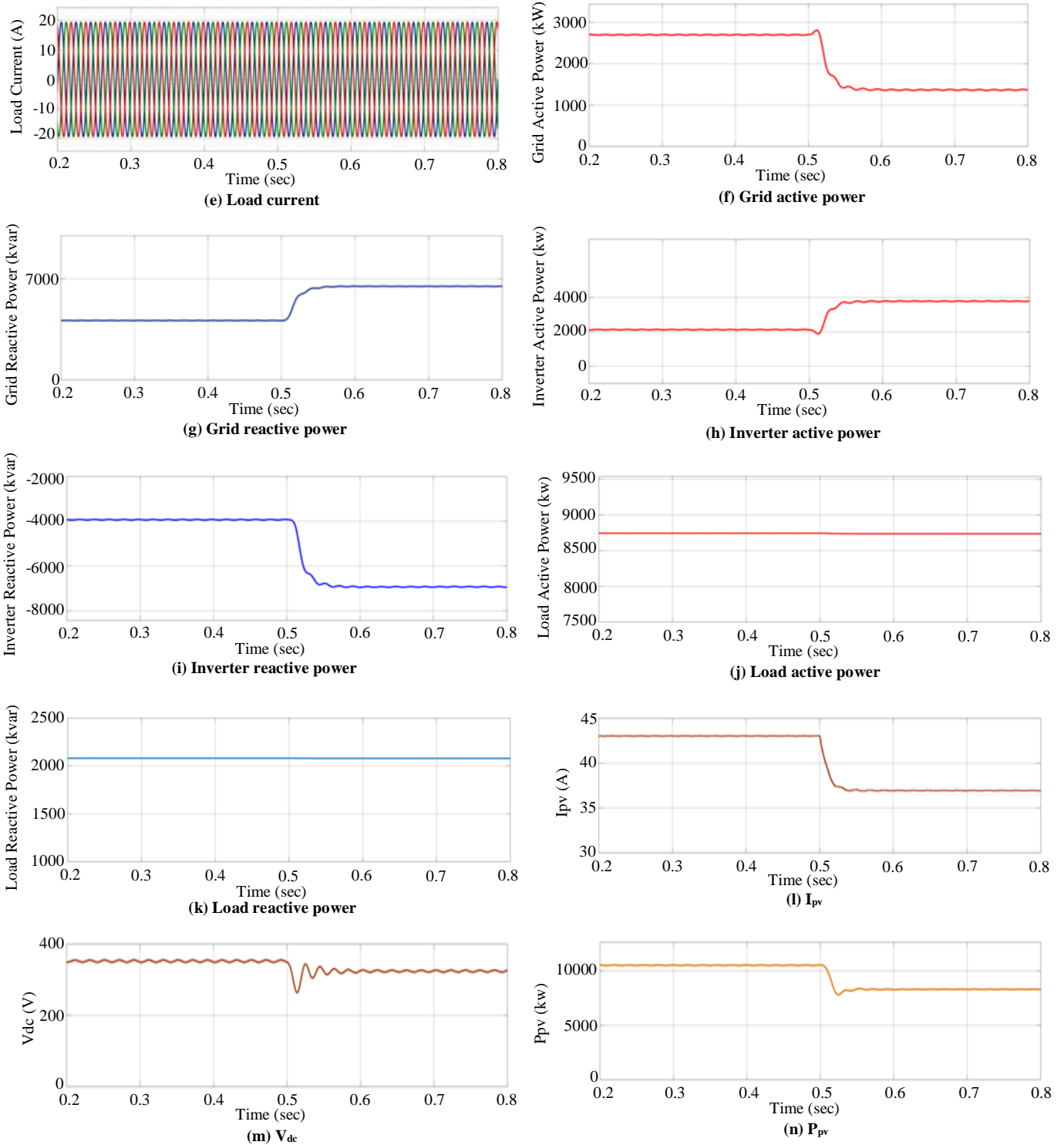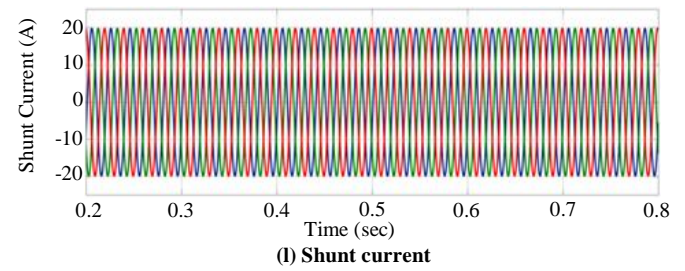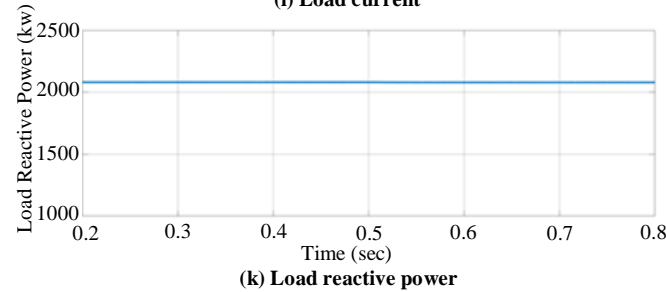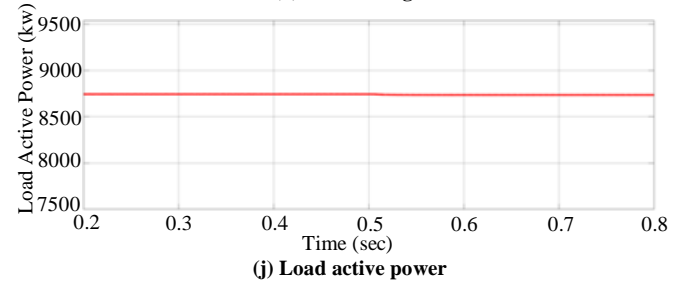

(a) Grid voltage

(b) Grid Current

(c) Inverter current

(d) Load voltage

(e) Load current

(f) Grid active power

(g) Grid reactive power

(h) Inverter active power

(i) Inverter reactive power

(j) Load active power

(k) Load reactive power
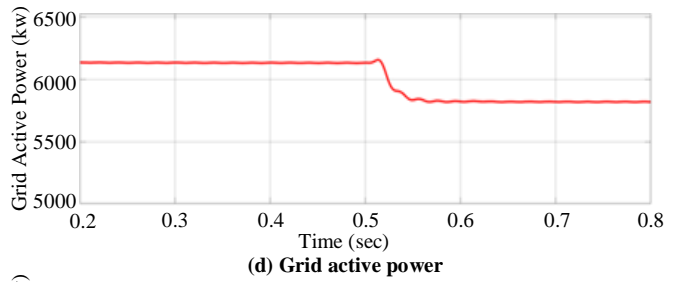
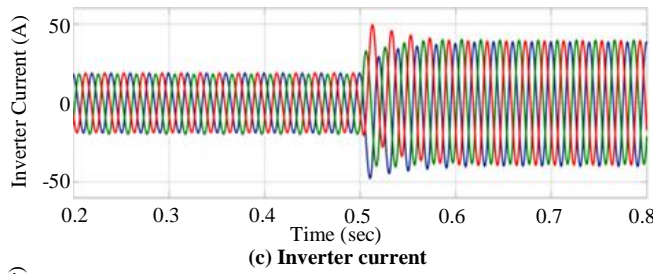**(l) I$_{pv}$**
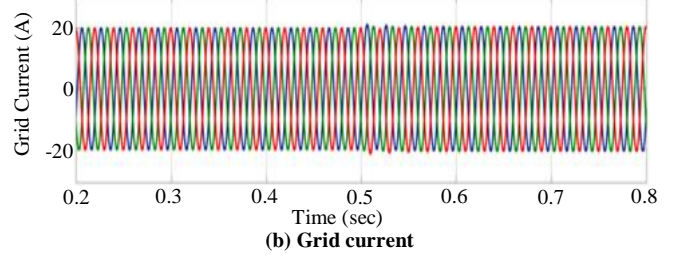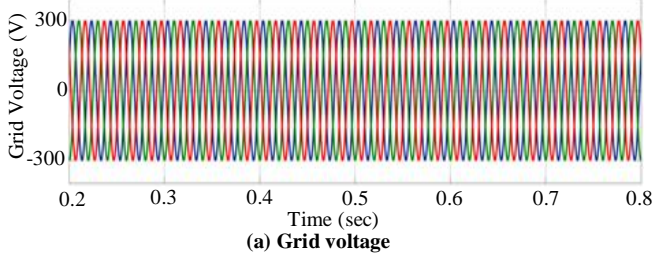
(m) V$_{dc}$

(n) P$_{pv}$

Fig. 13 Simulation results for PV-connected DC-AC boost inverter without STATCOM mode

6.2. Results for Grid Stability and Solar Power Generation under Variable Solar Irradiance with STATCOM Condition

(a) Grid voltage

(b) Grid current

(c) Inverter current

(d) Grid active power

(e) Grid reactive power

(f) Inverter active power

(g) Inverter reactive power

(h) Load voltage

(i) Load current

(j) Load active power

(k) Load reactive power

(l) Shunt current

(m) Shunt Vdc

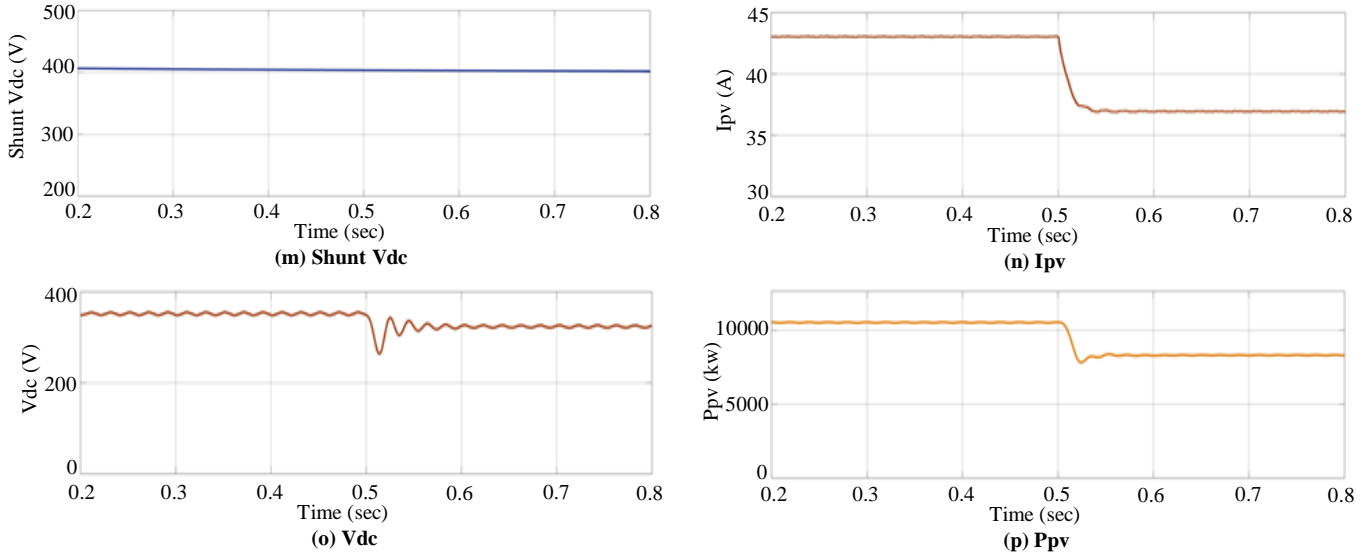**(n) Ipv**

(o) Vdc

(p) Ppv
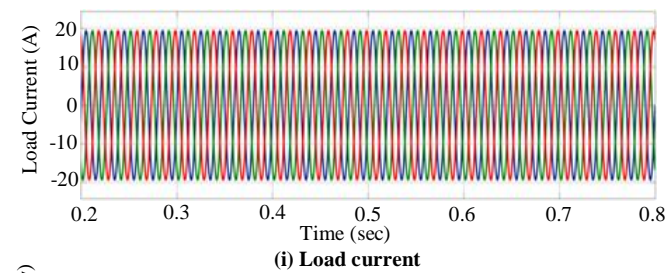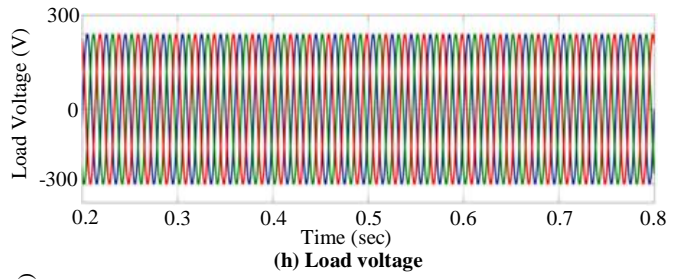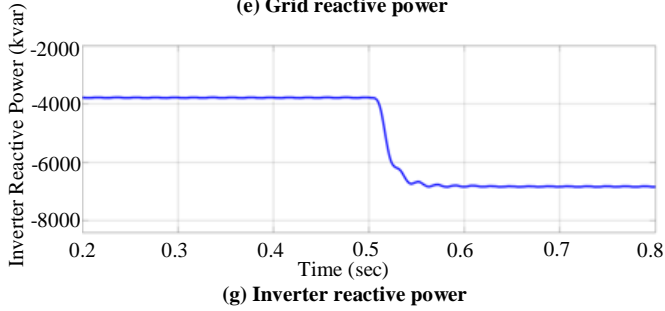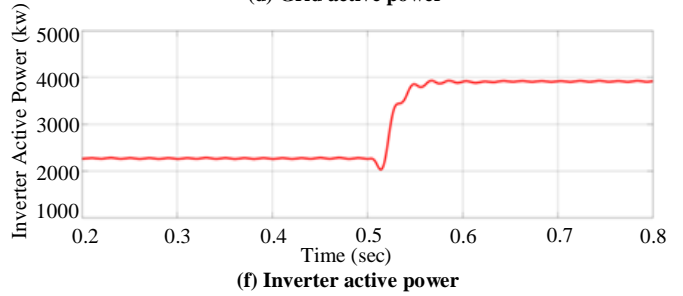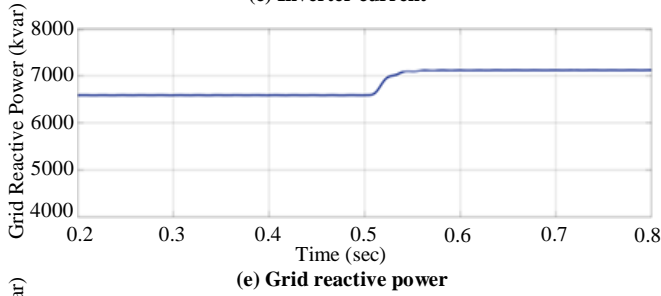
Fig. 14 Simulation results for PV connected DC-AC boost inverter with STATCOM mode

With and without a connected STATCOM device, the harmonic analysis of the proposed system reveals:

6.2.1. *Without STATCOM*

Harmonic evaluations of the proposed grid-connected PV system may be performed using Total Harmonic Distortion (THD) calculations without requiring a STATCOM device.

Using FFT analysis, we can show that the harmonics injected by the grid current and the load current result in a THD of 4.97% for the PV system with STATCOM and 30.19% without it (see Figure 15(a)).

6.2.2. *With STATCOM*

Harmonic analysis for a PV system connected to the grid through STATCOM may be calculated using Total Harmonic Distortion (THD). Using FFT analysis, we can show that the harmonics injected by the grid current and load current in the PV system with STATCOM device are 2.29% and 27.38%, respectively, in Figure 15(b). We find that grid-connected PV systems with and without a STATCOM device have differing Total Harmonic Distortion (THD) values, with the former having lower THD values. The following analysis demonstrates that the solar farm, as a PV-based STATCOM device, can completely mitigate the load's contribution to harmonic distortion.
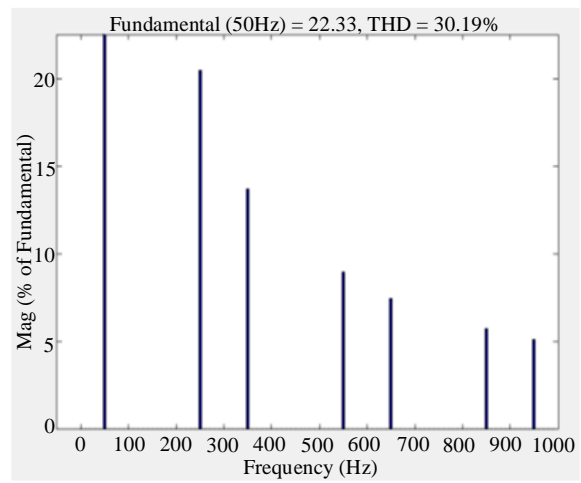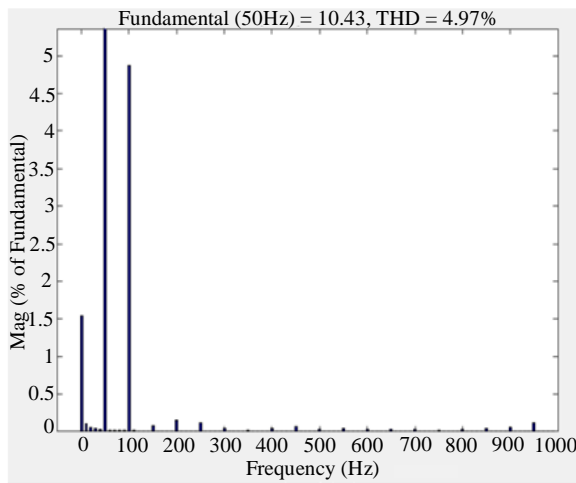

Fig. 15(a) Harmonic spectra of grid current and load current under without STATCOM condition
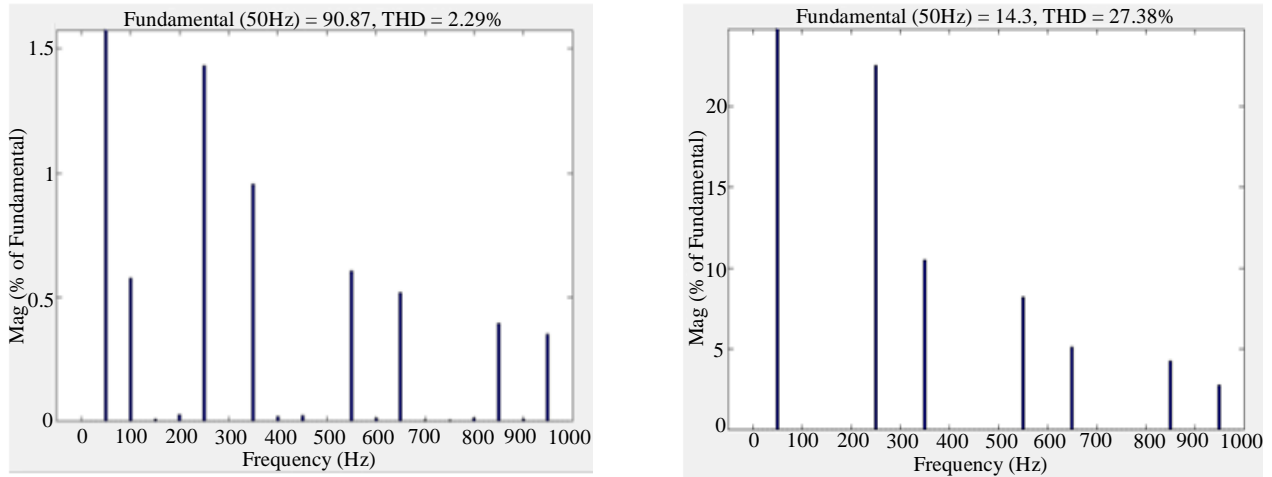
Fig. 15(b) Harmonic spectra of grid current and load current under with STATCOM condition

7. Conclusion

This paper proposes a six-switch design for a three-phase AC voltage much higher than the input DC voltage in a single power stage to convert a three-phase boost inverter. Three DC-DC boost converters about follower mode provide sinusoidal voltages for the proposed inverter.

The suggested system model is simulated in its entirety using MATLAB/Simulink. The photovoltaic solar array system linked to the grid has been tested under various conditions, including those where STATCOM modes for reactive power adjustment were enabled and those where they were not. The results of the simulations demonstrate that STATCOM effectively and dynamically adjusts the reactive power of the grid-connected solar PV array system in response to reactive power needs on the load side.

This research shows that the ANN-based DC-AC boost inverter and D-STATCOM effectively manage linear and non-linear loads connected to the grid. It has been shown that proficient control behaviour and quick responsiveness lower harmonics. Simulation results and a tabular comparison reveal that the proposed controller is superior to conventional approaches.

References

[1] L.I. Dong-hui et al., "Research on Several Critical Problems of Photovoltaic Grid-Connected Generation System," *Power System Protection and Control*, vol. 38, no. 21, pp. 208-214, 2010. [Google Scholar]

[2] Shi Jie, and AI Qian, "Research on Several Key Technical Problems in Realization of Smart Grid," *Power System Protection and Control*, vol. 37, no. 19, pp. 1-4, 2009. [Google Scholar]

[3] N. Kasa, T. Iida, and H. Iwamoto, "Maximum Power Point Tracking with Capacitor Identifier for Photovoltaic Power System," *2000 Eighth International Conference on Power Electronics and Variable Speed Drives*, London, UK, pp. 130-135, 2000. [CrossRef] [Google Scholar] [Publisher Link]

[4] Faruk Yalcin, "A Novel Three-Phase Buck-Boost Inverter Controlled by an Open-Loop Assisted Closed-Loop Hybrid Control Method," *International Journal of Circuit Theory and Applications*, vol. 49, no. 3, pp. 656-682, 2021. [CrossRef] [Google Scholar] [Publisher Link]

[5] F. Barzegar, and S. Cuk, "Solid-State Drives for Induction Motors: Early Technology to Current Research," *Proceedings of IEEE Region*, Anaheim, CA, vol. 6, pp. 15-18, 1982. [Google Scholar]

[6] F. Barzegar, and S. Cuk, "A New Switched-Mode Amplifier Produces Clean Three-Phase Power," *Proceedings Ninth International Solid-State Power Conversion Conference*, Washington, DC, 1982. [Google Scholar]

[7] R. Caceres, and I. Barbi, "A Boost DC–AC Converter: Operation, Analysis, Control and Experimentation," *Proceedings of IECON '95 - 21st Annual Conference on IEEE Industrial Electronics*, Orlando, FL, USA, pp. 546-551, 1995. [CrossRef] [Google Scholar] [Publisher Link]

[8] R. Caceres, and I. Barbi, "A Boost DC–AC Converter: Design, Simulation and Implementation," *Proceedings of Power Electronic Brazilian Conference (COBEP'95)*, pp. 509-514, 1995. [Google Scholar]

[9] R. Caceres, "*DC–AC Converters Family, Derived from the Basic DC–DC Converters*," Ph.D. Dissertation Thesis, Federal University of Santa Catarina, Brazil, 1997. [Google Scholar]

[10] Lina M. Elobaid, Ahmed K. Abdelsalam, and Ezeldin E. Zakzouk, "Artificial Neural Network-Based Photovoltaic Maximum Power Point Tracking Techniques: A Survey," *IET Renewable Power Generation*, vol. 9, no. 8, pp. 1043-1063, 2015. [CrossRef] [Google Scholar] [Publisher Link]

[11] Santi Agatino Rizzo, and Giacomo Scelba, "ANN Based MPPT Method for Rapidly Variable Shading Conditions," *Applied Energy*, vol. 145, pp. 124-132, 2015. [CrossRef] [Google Scholar] [Publisher Link]

[12] Byunggyu Yu, Mikihiko Matsui, and Gwonjong Yu, "A Review of Current Anti-Islanding Methods for Photovoltaic Power System," *Solar Energy*, vol. 84, no. 5, pp. 745-754, 2010. [CrossRef] [Google Scholar] [Publisher Link]

[13] F. Iov et al., "Power Electronics and Control of Renewable Energy Systems," *2007 7th International Conference on Power Electronics and Drive Systems*, Bangkok, Thailand, pp. 6-28, 2007. [CrossRef] [Google Scholar] [Publisher Link]

[14] Lie Xu, and Dong Chen, "Control and Operation of a DC Micro Grid with Variable Generation and Energy Storage," *IEEE Transactions on Power Delivery*, vol. 26, no. 4, pp. 2513-2522, 2011. [CrossRef] [Google Scholar] [Publisher Link]

[15] Rajiv K. Varma, and Ehsan M. Siavashi, "PV-STATCOM: A New Smart Inverter for Voltage Control in Distribution Systems," *IEEE Transactions on Sustainable Energy*, vol. 9, no. 4, pp. 1681-1691, 2018. [CrossRef] [Google Scholar] [Publisher Link]

[16] Rajiv K. Varma, and Reza Salehi, "SSR Mitigation with a New Control of PV Solar Farm as STATCOM (PV-STATCOM)," *IEEE Transactions on Sustainable Energy*, vol. 8, no. 4, pp. 1473-1483, 2017. [CrossRef] [Google Scholar] [Publisher Link]

[17] Rajiv K. Varma et al., "Harmonic Impact of a 20-MW PV Solar Farm on a Utility Distribution Network," *IEEE Power and Energy Technology Systems Journal*, vol. 3, no. 3, pp. 89-98, 2016. [CrossRef] [Google Scholar] [Publisher Link]

[18] Rajiv K. Varma, and Hesamaldin Maleki, "PV Solar System Control as STATCOM (PV-STATCOM) for Power Oscillation Damping," *IEEE Transactions on Sustainable Energy*, vol. 10, no. 4, pp. 1793-1803, 2019. [CrossRef] [Google Scholar] [Publisher Link]

[19] R.O. Caceres, W.M. Garcia, and O.E. Camacho, "A Buck-Boost DC-AC Converter: Operation, Analysis and Control," *6th IEEE Power Electronics Congress. Technical Proceedings*, Morelia, Mexico, pp. 126-131, 1998. [CrossRef] [Google Scholar] [Publisher Link]

[20] Golam Sarowar, Mohammad Ali Choudhury, and Md. Ashraful Hoque, "A Novel Control Scheme for Buck-Boost DC to AC Converter for Variable Frequency Applications," *Procedia - Social and Behavioral Sciences*, vol. 195, pp. 2511-2519, 2015. [CrossRef] [Google Scholar] [Publisher Link]

[21] Chandan Kumar, and Mahesh K. Mishra, "A Voltage-Controlled DSTATCOM for Power-Quality Improvement," *IEEE Transactions on Power Delivery*, vol. 29, no. 3, pp. 1499-1507, 2014. [CrossRef] [Google Scholar] [Publisher Link]

[22] Jawad Hussain et al., "Power Quality Improvement of Grid Connected Wind Energy System Using DSTATCOM-BESS," *International Journal of Renewable Energy Research*, vol. 9, no. 3, pp. 1388-1397, 2019. [CrossRef] [Google Scholar] [Publisher Link]

[23] Ambarnath Banerji, Sujit K. Biswas, and Bhim Singh, "DSTATCOM Control Algorithms: A Review," *International Journal of Power Electronics and Drive Systems (IJPEDS)*, vol. 2, no. 3, pp. 285-296, 2012. [Google Scholar] [Publisher Link]

[24] Snehasish Bansriar, and Roshan Nayak, "Modeling of Adaptable Voltage Controller and Its Stability Analysis in Distributed Generation System," *International Journal of Current Engineering and Technology*, vol. 5, no. 3, pp. 1798-1801, 2015. [Google Scholar] [Publisher Link]

[25] Zhou Ming et al., "Control Method for Power Quality Compensation Based on Levenberg-Marquardt Optimized BP Neural Networks," *2006 CES/IEEE 5th International Power Electronics and Motion Control Conference*, Shanghai, China, pp. 1-4, 2006. [CrossRef] [Google Scholar] [Publisher Link]

[26] Hao Yu, and Bogdan M. Wilamowski, *Levenberg–Marquardt Training*, Intelligent Systems, 1st ed., CRC Press, 2011. [Google Scholar] [Publisher Link]